MULTISTAGE OPTIMIZATION OF AUTOMOTIVE CONTROL ARM THROUGH TOPOLOGY AND SHAPE OPTIMIZATION.

[1]Duane Detwiler, [2]Emily Nutwell*, [2] Deepak Lokesha

[1]Honda R&D Americas, USA, [2]Ohio State University SIMCenter, USA, [2]BETA CAE Systems USA Inc., USA,

KEYWORDS –
Optimization, Topology, Shape, Multi-stage, Morphing

ABSTRACT –
The ever-evolving nature of the global automotive industry brings about exciting challenges for the new age designers. The trends in the overall production costs, fuel costs and the awareness of environmental effects are some of the many factors that drive today's automotive design strategies. Use of optimization methodologies early on in design process has been adopted widely to achieve low cost and efficient component designs.

This paper discusses a multi-stage optimization methodology to reduce the time required in identifying an optimized concept design for a chassis component. As a first stage, a topology optimization is performed on a vehicle control arm design using LS-TaSC™ (LSTC). The loading condition applied to the design space represents a highly nonlinear load scenario similar to that seen during a crash event in the vehicle. The "topology-optimized design" is then subjected to a shape optimization. ANSA™'s (BETA CAE) morphing technology is used to define the shape change parameters on an LS-DYNA™ load case model. An ANSA™ – LS-OPT™ link is then created through the ANSA™ Task Manager. This allows for easy creation of linkages between the LS-OPT™ design variables and ANSA™morphing parameters. A minimization objective is selected for overall reduction in mass while maintaining necessary performance targets. The paper will present results and highlight the benefits of a multi-stage optimization strategy.

1. INTRODUCTION

The use of commercially available optimization tools has expanded greatly in industry in the past few years, particularly in the field of automotive design. Several optimization tools are now readily available to the engineer such as topology and shape optimization. These tools lend themselves to different stages of the design process. In particular, topology optimization is applied early in the design process in order to determine the optimum layout of the material for a defined design space and loading condition(s). In contrast, shape optimization is applied to a well-developed structure and is well suited to finding an optimum of this structure for a defined loading condition and constraints. Used in conjunction with each other, the structure can be developed from very early stages in which the engineer defines a design space and required loading conditions, to a fine-tuning of the structure, which results in a mature design. This process, which implements multiple optimization techniques, will lead to a more efficient structure for the defined loading conditions.

For this investigation, a vehicle control arm subjected to a nonlinear loading scenario is studied. A topology optimization is performed on the design space for this control arm using LS-TaSC. LS-TaSC is a topology optimization software available through LSTC which works with LS-DYNA as the finite element solver. LS-TaSC provides a user interface for the HCA algorithm (Hybrid Cellular Automata) which efficiently handles nonlinear loading during topology optimization. This structure is then the basis for a shape optimization where several morph boxes are defined in ANSA. These parameters are then linked to LS-OPT where constraints and mass minimization is defined. The final structure shows that applying shape optimization to the topology results in greater mass reduction while maintaining design requirements.

A description of the topology optimization methodology is described in the following section. The control arm model and loading condition are then detailed. Topology results and an interpretation of the results are discussed. The shape optimization where ANSA and LS-OPT are used jointly is explained in the following section. A discussion of the results and the challenges encountered during this project will follow. The paper will then conclude with a summary.

2. TOPOLOGY OPTIMIZATION METHOD

Historically, topology optimization in the field of crashworthiness has been a difficult challenge. Typically, topology optimization solves problems with elastic materials and static loading conditions using a minimization objective such as minimum compliance. However, this approach will not adequately solve for a structure that is efficient for crashworthiness. In this case, in addition to structural integrity, energy absorption is a desired characteristic. With this in mind, calculating the internal energy density (IED) of a structure can be expressed as

$$U = U^e + U^p = \int_0^{ef} \sigma de \qquad (1)$$

where the stress σ is integrated from the undeformed state to the final state due to loading. For a nonlinear problem where energy-absorbing characteristics are an important consideration of the structure, the idea is to maximize the area under the force-displacement curve for a defined loading hence maximizing the energy absorbed by the structure.

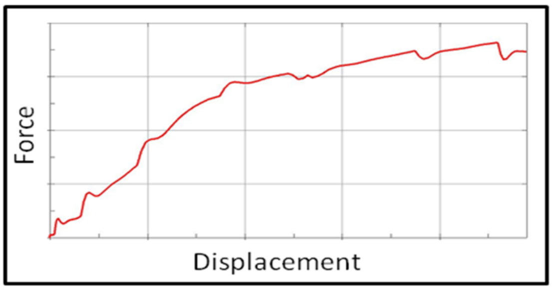

Fig.1: The area under the force stroke curve represents energy absorption.

Density based methodologies are often applied for topology optimization. The design space is represented with a finite element mesh and a design variable is assigned to each element. For this methodology, the relative densities is the design variable

$$\rho_i(x_i) = x_i \rho_0 \qquad 0 < x_i \leq 1 \qquad (2)$$

where ρ_0 is the density of the base material. Since nonlinear material properties must be considered, a piecewise linear material model is needed to represent the behavior of the aluminium material. The finite element analysis model is nonlinear; therefore, the design variable not only controls the density ρ of the material, but also the elastic modulus (E), the yield stress (σ_y) and the strain hardening modulus (E_h).

$$E_i(x_i) = x_i E_0 \qquad (3)$$

$$\sigma_i(x_i) = x_i \sigma_0 \qquad (4)$$

$$E_{h_i}(x_i) = x_i E_{h_0} \qquad (5)$$

In order to avoid intermediate material properties, a power law approach, the Solid Isotropic Material with Penalization (SIMP) approach is implemented. The material properties of the material, such as the Young's modulus, is interpolated as

$$E_i(x_i) = x_i^p E_0 \qquad (6)$$

where *p* is a penalization parameter which drives away intermediate densities from the topology solution.

The topology results are calculated using the Hybrid Cellular Automaton Method (HCA). This method is not explicitly an optimization technique; however, by using the local rules, an optimized solution is derived. The local rules operate according to local information collected in the neighbourhood of each cell of the CA (Celluar Automaton) lattice so that the average structural performance of the element itself as well as its neighbours is measured [3]. The HCA method strives to achieve a uniform distribution of a field variable. Here, the field variable is the internal energy density (IED) of the structure. This is achieved by minimizing the deviation from a set point

$$x_i^{new} = x_i + K_p(S_i + S^*) \quad (7)$$

where K_p is a scaling parameter, S_i is the field variable and S^* is the field variable set point. When the change of the structure is approximating zero, the field variable, which is the IED of the structure, is more uniformly distributed. In this way, the energy absorbed by the structure defined by the design space is maximized, generating an optimized structure for nonlinear loading scenarios.

3. MODEL OF VEHICLE CONTROL ARM

In this work we consider the optimization of a vehicle control arm structure. The load case defined for the topology optimization results in yielding of the part. For this loadcase, the desired topology optimization objective is to maximize the energy absorbed by the structure.

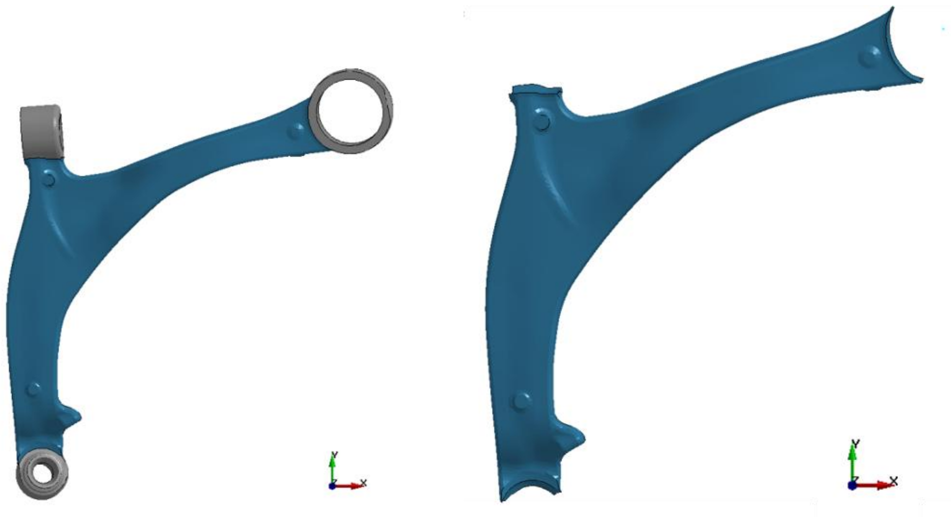

Fig.2: The LS-Dyna control arm model (left) and the design space for the optimization (right).

The control arm has a total mass of 4.025 kg of which the full density design space is 3.506 kg. There is one nonlinear load case defined (Fig. 3) where the control arm is subjected to a prescribed displacement in the x-direction from 0 to 110mm within 200ms. The volume connecting the bushing mounts of the control arm is defined as the design space for the topology optimization. The volume of the entire control arm structure including the design space is meshed using tetrahedral elements with a mesh size of 3 mm nominal. The material of the control arm design space as well as the suspension and chassis at the ends are modelled with a piecewise linear elastic-plastic aluminium material model represented with ***MAT24**. This model represents a laboratory test designed to ensure that the suspension components meet a minimum load requirement. This laboratory test is inspired by extreme loading conditions to the suspension system of the vehicle. A test fixture is mounted to the wheel hub, and a chain attaches the test fixture to a loading actuator which then applies the load. The relevant suspension components (damper, tie rod, knuckles) are modelled using a simplified beam representation in order to model realistic boundary conditions. The rubber bushings of the model are represented with solid elements using ***MAT_181_SIMPLIFIED_RUBBER/FOAM**. Although this controlled laboratory test is not inspired by any crash requirement, it provides a simple but ideal load case for the objective of maximizing energy absorption. This model is analyzed using LS-DYNA explicit.

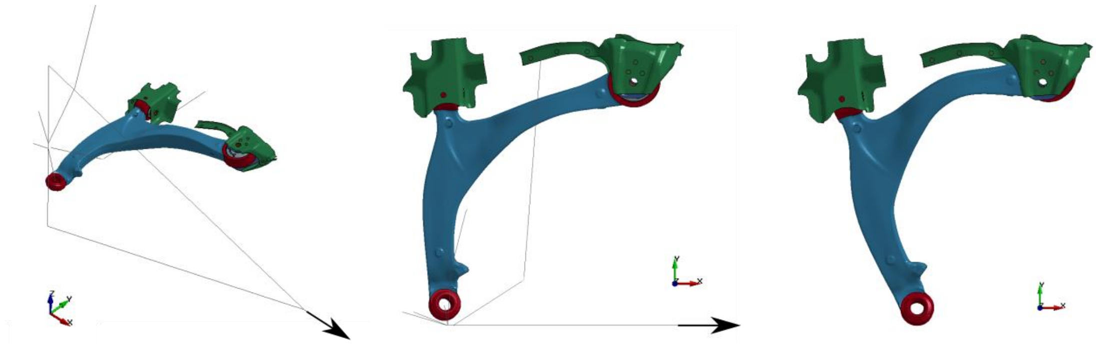

Fig.3: The LS-Dyna model of the nonlinear load case of the control arm. A prescribed displacement is applied to the chain. The rightmost figure shows the deformed structure when the load is applied to the full design space.

4. TOPOLOGY OPTIMIZATION

The objective for the topology optimization for the defined load case is maximizing energy absorption. The topology optimization is conducted using LS-TaSC which is the topology software designed to work with LS-DYNA. LS-TaSC provides a user interface for the HCA algorithm described in Section 2. A volume fraction of 0.49 is defined for the design space to achieve a mass target of 1.718 kg.
Initially, the topology evolved too quickly allowing for large changes in the structure between iterations. This is a concern because if too much material is removed too quickly, instabilities can occur which can results in unwanted contact behavior, large changes in deformation modes, and possible error termination of the finite element model. In this case, large differences in the structure are noted between the fourth and fifth iteration with the defined mass fraction as shown in Figure 4.

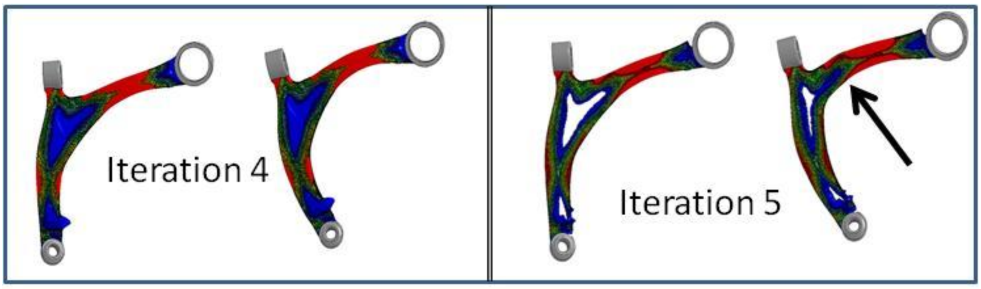

Fig.4: The topology structure at Iteration 4 and Iteration 5 with default move limit = 0.1. Contact penetration is noted in iteration 5.

The amount of material removed in iteration 5 results in a remarkably different deformation mode and contact instabilities were noted. The intermediate density elements have a very low stiffness resulting in challenging contact issues, and penetration is noted which is nonphysical. This can lead to instabilities, or topology results that are evolved based on nonphysical deformation modes.
In order to account for this, LSTC implemented a feature in LS-TaSC where the move limit can be adjusted. In the previous result, instabilities arose because the material changed too quickly between iterations. The update rule can be expressed as:

$$\Delta x_i^{(k)} = \max\{-0.1, \min\{K_p(\overline{S}_i^{(k)} - S_i^{*(k)}), 0.1\}\}. \qquad (8)$$

Therefore, the maximum allowable change in relative density is 0.1. However, in this case, 0.1 proved to be too large to develop a stable topology result; therefore, the move limit is changed from 0.1 to 0.02. This will result in the topology solution evolving more slowly requiring more iterations to converge. This computational cost must be weighed against the stability of the topology results.

The settings LS-TaSC are called out in Table 1.

HCA Parameter (LS-TaSC Setting)	Parameter Value
Mass Fraction	0.49
Minimum Length Scale (Neighbor Radius)	9mm
Move Limit	0.02
Convergence tolerance	0.002

Table 1: Applied LS-TaSC Parameters

The objective of energy absorption is calculated by measuring the force in the chain and integrating it over the stroke. The loading and results of the topology is shown in Figure 5.

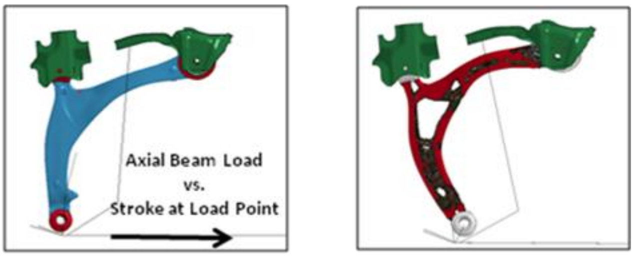

Fig.5: The topology loading and results.

4.1 TOPOLOGY RESULTS FOR SHAPE OPTIMIZATION

In order to apply the topology results for a shape optimization, post processing of the topology results is necessary so that the results are represented by a uniform density structure. This post processing was done manually in an iterative fashion, which was very time consuming; therefore, the process will not be detailed here. A smooth shape is interpreted from the topology results, and the force stroke curves are compared to ensure that the smooth arm is an "equivalent" structure to the topology results with respect to the topology objective of energy absorption. Since this is measured by integrating the force stroke curves, this data is the metric used to compare the two structures as shown in Figure 6.

Fig.6: The topology results compared to the smooth arm structure as a result of manual post processing. The comparison of the force strokes curves is shown to the right.

The deformed shape of the topology result and the smooth arm is also compared to ensure adequate similarities between the structures. This comparison is shown in Figure 7.

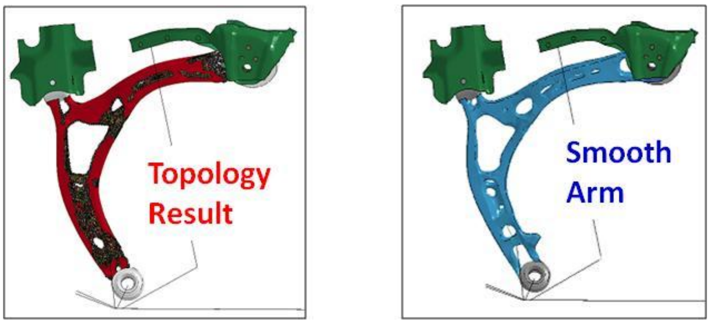

Fig.7: The topology results compared to the smooth arm structure as a result of manual post processing: deformed shapes are similar.

The post processing of the topology results shows comparable performance to the topology results. Therefore, the smooth structure is a good representation of the topology results and will be used for further optimization using shape optimization techniques.

5. SHAPE OPTIMIZATION PARAMETERIZATION IN ANSA

Once the topology results are available, further improvements can be made to the design by the application of shape optimization. Additionally, as a result of the post processing necessary to represent the topology results as a smooth, uniform density model, there tends to be a shift away from the optimized point in the design space. The shape optimization stage is necessary to minimize the effects of such shifts and to improve upon the topology results in order to acheive a truly optimized design.

To create the model for shape optimization, some areas of the model are identified for shape changes (morphing) using the ANSA pre processor's morphing technology. The areas intended for morphing are contained in morphing boxes. Figure 8 shows the structure of morphing boxes constructed to encompass the desired areas of interest.

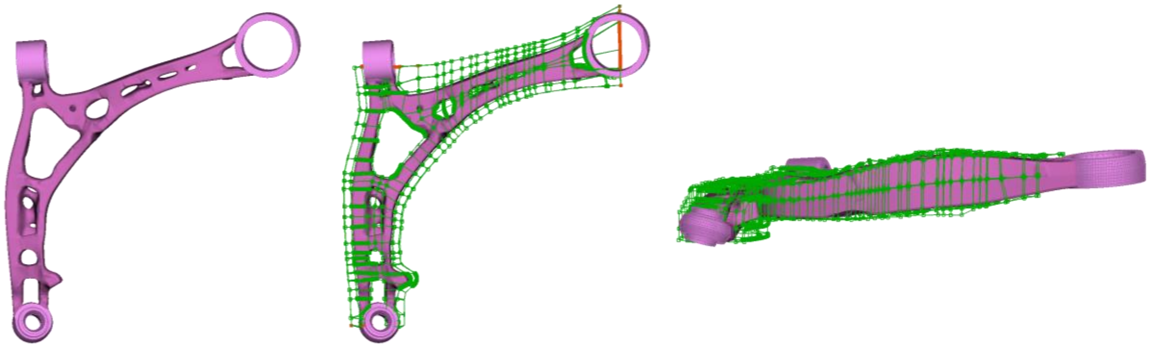

Fig.8: The morphing boxes created to include areas for shape changes.

Each of these hexagonal boxes includes handles defined for movements (morphing) which are referred to as control points. The movements of these control points in 3-D space affect the shape of the boxes and in turn the entities contained within them. This induces local changes in the shape for the control arm.

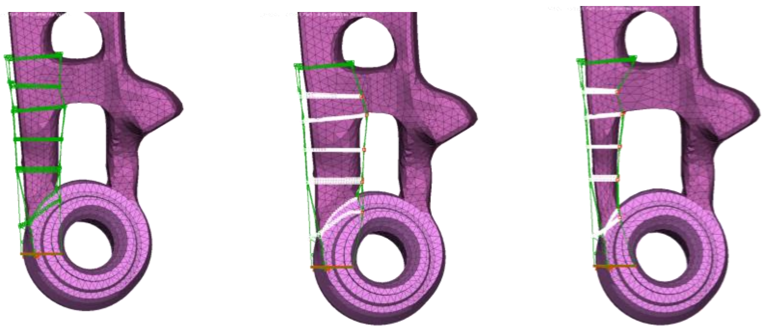

Fig.9: Unidirectional morphing parameter to change thickness of a region.

These morphing operations are parameterized using the ANSA morph parameters. A few such examples are shown in Figure 9 & 10 to showcase the intended effects brought about on the control arm with the change in values of the morph parameters.

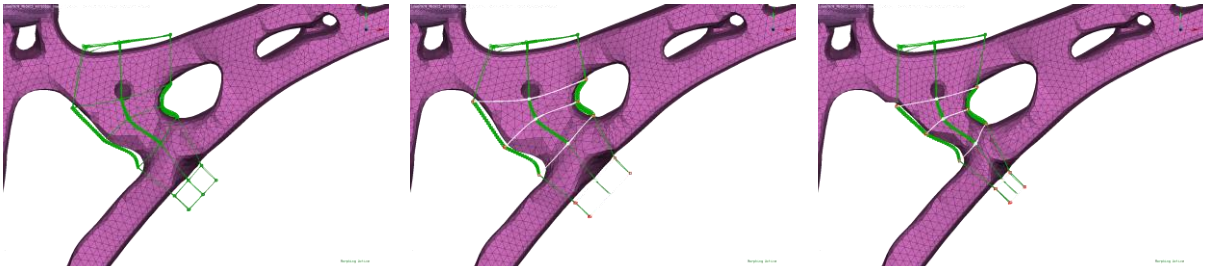

Fig.10: Multidirectional morphing parameter to change thickness of a region.

In this model, a total of 31 such morphing parameters *(Appendix A)* are created to provide very specific control over the shape change operations. An optimization task created in the ANSA Task Manager tool is used to link these parameters to the LS-OPT optimizer code as design variables. The Task Manager is also used to assign individual constraint space for each design variable. There are tasks in place to manage the mesh quality in cases where the morphing operation creates distortions in original model. A meshing task is included to automatically generate solid meshes for each model status. The output from the ANSA Task Manager is a completely defined LS-DYNA model.

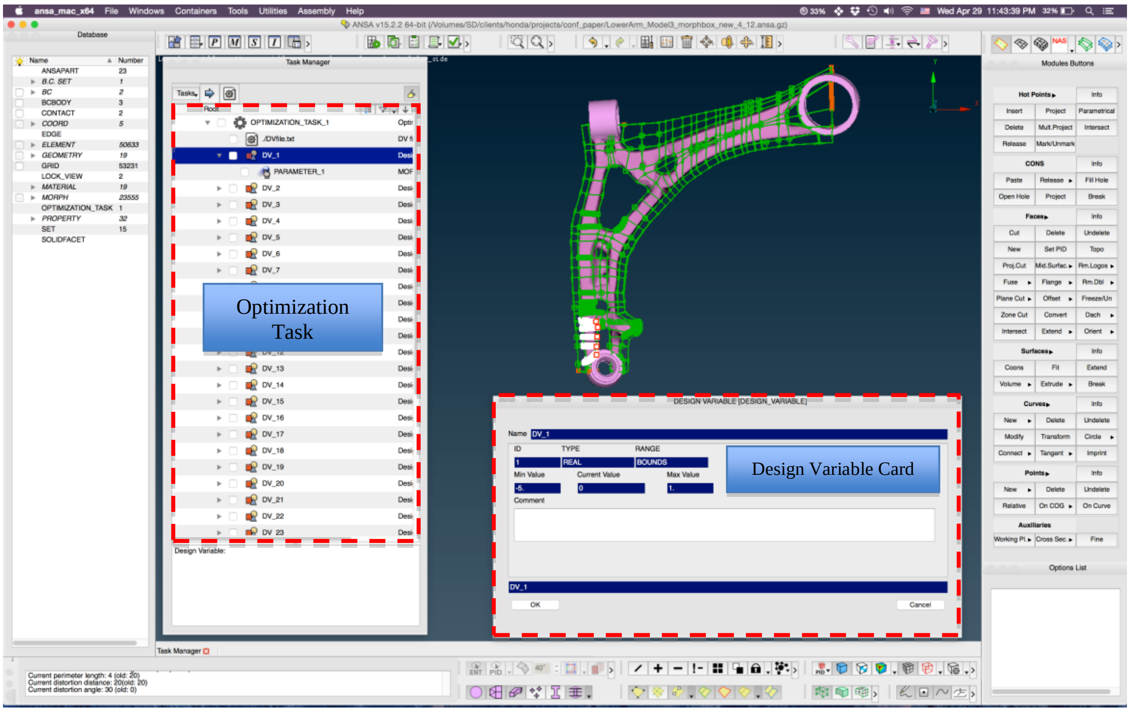

Fig.11: ANSA Task Manager with Optimization task to link morph parameters to LS-OPT design variables.

Based on the parameterized model, a design of experiments (DOE) study is conducted. A simple Space – Filling method is used to create 50 samples. This ensures a good representation of the design space while limiting the need for a large number of samples. Particular consideration is placed on reducing the overall computational resources and human time required to generate a response surface. Prior to executing the LS-DYNA runs, the simulate function in the ANSA Task Manager is used to determine potential failure samples. If necessary, the morphing boxes are adjusted such that each sample will result in a running LS-DYNA file in order to eliminate erroneous results. This critical step is necessary to make this process economically viable while being technically relevant.

6. SHAPE OPTIMIZATION: LS-OPT

The LS-OPT optimization setup is created as shown in Figure 12. LS-OPT is programmed to call in an ANSA module to link the ANSA file containing the morphed model. It is also able to decipher the ANSA generated DV (Design Variable) file and auto load the design variables into LS-OPT. LS-OPT then updates the DV file based on the sampling data to execute the ANSA module and create the design of experiment models and submit them to LS-DYNA for solution.
The responses and constraints are defined using LS-DYNA output. The objective for the shape optimization is defined to minimize the mass of the structure. In order to maintain structural integrity, a minimum load in the chain is defined as a constraint. Also, a maximum plastic strain is defined in order for the shape optimization to generate a robust structure.

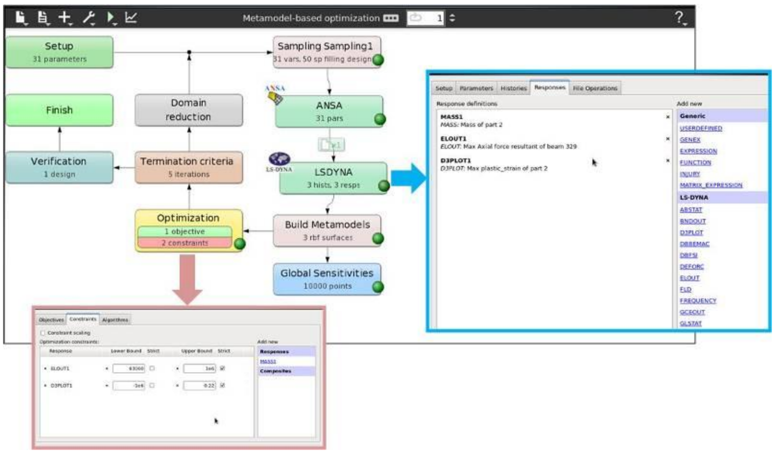

Fig.12: The LS-OPT Database for shape optimization. The LS-DYNA parameters and the constraints are detailed.

The accuracy plots show that although the force and minimum mass values are well predicted by the meta model defined, the plastic strain show significant noise. This can be traced back to several issues including the manual post processing that was used to generate the smooth model of the lower arm needed for the shape optimization. This problem is highlighted when the confirmation run violates the plastic strain constraint resulting in the computed optimum not meeting the plastic strain requirement.

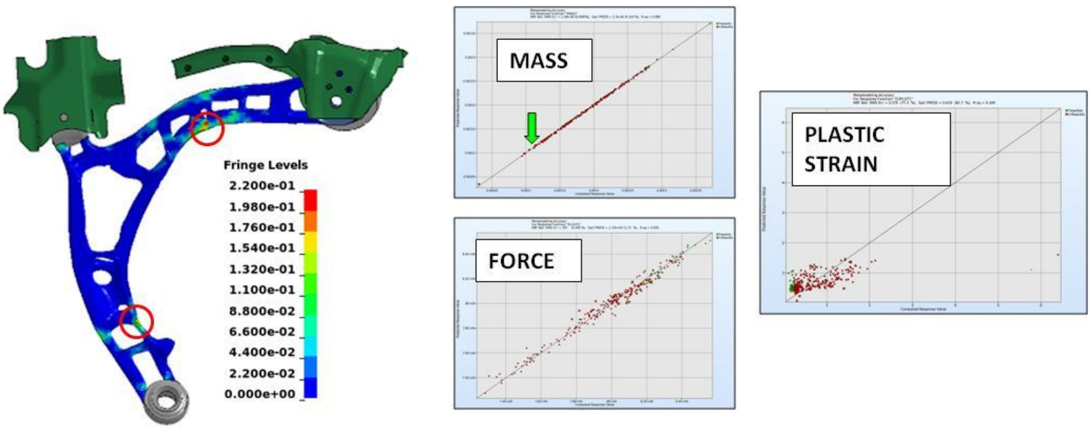

Fig.13: The calculated optimum arm shows violations of the plastic strain constraint. The accuracy plots indicate that although the mass objective and force constraint are well predicted; the plastic strain constraint is not. The arrow in the mass plot indicates the "best" feasible simulation run (lowest mass and all constraints satisfied).

For purposes of this investigation, the "best" simulation point (i.e. lowest mass) which is feasible will be used as the result of the shape optimization rather than the calculated optimum which violates the plastic strain constraint. This point is indicated in the mass plot in Figure 13. Although this is not a true optimum, it is sufficient to validate the process of using topology and shape optimization in tandem with each other.

Figure 14 shows the results of the shape optimization compared to the smooth arm that is derived from the topology optimization. Overall, the shape optimization results in an 11% reduction in mass of the design space.

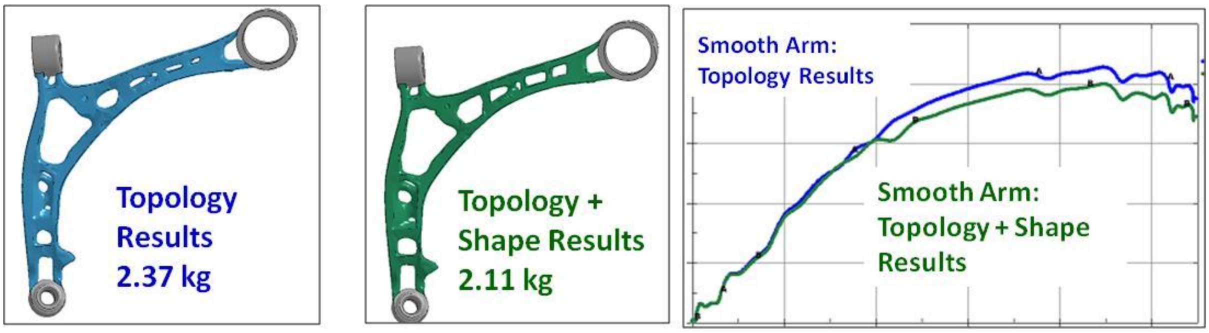

Fig.14: The results of the arm derived from topology optimization only and topology + shape optimization. The shape optimization results in an 11% reduction in mass while achieving all constraints defined for the control arm performance as shown in the force-stroke curves.

7. CONCLUSIONS

In this paper, a process is outlined to combine topology optimization with shape optimization in order to evolve a design of a suspension control arm with minimized weight while achieving performance targets. Topology optimization is conducted on a design space which would be available early in the development flow. Post processing of the topology results is necessary in order to apply shape optimization to this design. This is a potential area of future research since this was done manually and was not an efficient process. This manual process also results in difficulties for the morphing during the shape optimization. Combining shape optimization with topology optimization results in an 11% reduction in mass over application of topology optimization alone. Therefore, this investigation successfully showcases the application of topology and shape optimization to generate an optimal structure which meets defined design requirements.

7. ACKOWLEDGEMENTS

We thank Willem Roux from LSTC for his continuing support, particularly with regard to the implementation of the variable move limit functionality in LS-TaSC. We also thank Imtiaz Gandikota from LSTC for his support with LS-OPT.

REFERENCES

(1) ANSA version 12.1.5 User's Guide, BETA CAE Systems S.A., July 2008
(2) Patel, N. M.: "Crashworthiness design using topology optimization", Ph. D. thesis, University of Notre Dame, 2007.
(3) Patel, N. M., Kang, B.-S., Renaud, J. E. and Tovar, A.: "Crashworthiness design using topology optimization", Journal of Mechanical Design 131, 2009, 061013.
(4) Livermore Software Technology Corporation: "The LS-TaSC™ Software, Topology and Shape Computations Using the LS-Dyna Software, User's Manual", Version 3.0, from: www.lspoptsupport.com, 2013.
(5) Livermore Software Technology Corporation: "The LS-OPT™ User's Manual A Design Optimization and Probabilistic Analysis Tool for the Engineering Analyst", Version 5.0, from: www.lspoptsupport.com, 2013.
(6) Aulig, N., Nutwell, E., Menzel, S., Detwiler, D.: "Towards multi-objective topology optimization of structures subject to crash and static load cases", Engineering Optimization 2014, CRC Press, 2014, 847-852.

(7) Olason, A., Tidman D.: Methodology for Topology and Shape Optimization in the Design Process", Master's Thesis, Chamlers University of Technology, 2010.

(8) Bendsøe, M.: "Optimization of Structural Topology, Shape, and Material", Springer Verlag Berlin Heidelberg New York, 1995.

(9) Roux, W.: "Topology design using LS-TaSC™ version 2 and LS-DYNA", 8th European LS-DYNA Users Conference, 2011.

(10) Livermore Software Technology Corporation: "The LS-DYNA™ Keyword User's Manual" Vol I and II, LS-DYNA R7.1, from: www.lstc.com/download/manuals, 2014.

(11) μETA PostProcessor version 6.2.0. User's Guide, BETA CAE Systems S.A., June 2008

APPENDIX A:

```
#
# DESIGN VARIABLES
#-----------------------------------------------------------------------------------------
# ID | DESIGN VARIABLE NAME | TYPE | RANGE | CURRENT VALUE |  MIN VALUE -->  MAX VALUE | STEP
#-----------------------------------------------------------------------------------------
 1,  DV_1,  REAL,     BOUNDS,    0., -5., 1.
 2,  DV_2,  REAL,     BOUNDS,    0., -5., 1.
 3,  DV_3,  REAL,     BOUNDS,    0., -5., 1.
 4,  DV_4,  REAL,     BOUNDS,    0., -1., 1.
 5,  DV_5,  REAL,     BOUNDS,    0., -5., 1.
 6,  DV_6,  REAL,     BOUNDS,    0., -5., 1.
 7,  DV_7,  REAL,     BOUNDS,    0., -1., 1.
 8,  DV_8,  REAL,     BOUNDS,    0., -5., 1.
 9,  DV_9,  REAL,     BOUNDS,    0., 0., 3.
 10,  DV_10,  REAL,     BOUNDS,    0., -3., 1.
 11,  DV_11,  REAL,     BOUNDS,    0., -2., 1.
 12,  DV_12,  REAL,     BOUNDS,    0., -2., 1.
 13,  DV_13,  REAL,     BOUNDS,    0., -5., 1.
 14,  DV_14,  REAL,     BOUNDS,    0., -5., 1.
 15,  DV_15,  REAL,     BOUNDS,    0., -5., 1.
 16,  DV_16,  REAL,     BOUNDS,    0., -5., 1.
 17,  DV_17,  REAL,     BOUNDS,    0., -5., 1.
 18,  DV_18,  REAL,     BOUNDS,    0., -5., 1.
 19,  DV_19,  REAL,     BOUNDS,    0., -5., 1.
 20,  DV_20,  REAL,     BOUNDS,    0., -5., 1.
 21,  DV_21,  REAL,     BOUNDS,    0., -5., 1.
 22,  DV_22,  REAL,     BOUNDS,    0., -7., 0.5
 23,  DV_23,  REAL,     BOUNDS,    0., -15., 1.
 24,  DV_24,  REAL,     BOUNDS,    0., -5., 1.
 25,  DV_25,  REAL,     BOUNDS,    0., -5., 1.
 26,  DV_26,  REAL,     BOUNDS,    0., -5., 1.
 27,  DV_27,  REAL,     BOUNDS,    0., -5., 1.
 28,  DV_28,  REAL,     BOUNDS,    0., -5., 1.
 29,  DV_29,  REAL,     BOUNDS,    0., -5., 1.
 30,  DV_30,  REAL,     BOUNDS,    0., -1., 1.
 32,  DV_32,  REAL,     BOUNDS,    0., -5., 1.
#-----------------------------------------------------------------------------------------
```

Table A: Design Variables and constraints space